UNCLASSIFIED

AD 414673

DEFENSE DOCUMENTATION CENTER

FOR

SCIENTIFIC AND TECHNICAL INFORMATION

CAMERON STATION, ALEXANDRIA, VIRGINIA

UNCLASSIFIED

G: - 4 - 5

R63SD61

STUDY OF STRESSES NEAR A DISCONTINUITY IN A FILAMENT-REINFORCED COMPOSITE METAL

N.F. DOW

SPACE SCIENCES LABORATORY

GENERAL ✦ ELECTRIC

MISSILE AND SPACE DIVISION

SPACE SCIENCES LABORATORY

MECHANICS SECTION

STUDY OF STRESSES NEAR A DISCONTINUITY IN A
FILAMENT-REINFORCED COMPOSITE METAL*

By

Norris F. Dow

R63SD61
August 1963

MISSILE AND SPACE DIVISION

GENERAL ELECTRIC

CONTENTS

SUMMARY

A study is made of stresses in the vicinity of discontinuities in fialments in filament-reinforced, composite materials. Formulas are derived for the calculation of local stresses in filament or binder, and for the shear stresses induced between them. Sample calculations (in both elastic and plastic stress ranges) show that disturbances from the general stress level are primarily local, near the discontinuity, and particularly that the shear stress between fiber and binder is apt to rise to a high peak value at the discontinuity. The magnitude of this peak is shown to be governed by a parameter λ, defined in the report, which also governs the length of filament required to approach infinite length in effectiveness. Thus any attempts to reduce the shear stress, as by permitting yielding of the binder, will also increase the filament length required for effective reinforcement. The conclusion is reached that the accommodation of the high peak shear stresses at discontinuities may well be the crux of the attainment of the potentials apparently available with high-strength filaments or "whiskers" as reinforcements for composite materials.

INTRODUCTION

The mechanism of load transfer between filament and binder in a
filament-reinforced, composite material is of interest because of the
desirability of utilizing the potential strength of available filaments or
"whiskers" for structural materials. Especially since some whiskers
are available only in short lengths, a determination of the length required
for reinforcing effectiveness should be helpful in guiding the development
of composites. Clearly if short filaments are to be effective, they must
pick up the stresses which they are to carry near their ends, so that the
short, individual filaments can behave in the same manner as long,
continuous elements.

By analogy to the problems of "shear lag" in structures, the
probability seems good that the whisker may not need to be very long to
act essentially as if it were of infinite length. Experimentally, Jech,
McDanel and Weeton (ref. 1) seemed to find that such could be the c .e.
Parratt on the other hand (ref. 2) by a novel indirect approach reasoned
that lengths of the order of 1000 whisker diameters are required to
approach the action of a long filament.

In this paper, an analysis is made of the stresses in the vicinity of
a discontinuity in reinforcing filaments. The elastic analysis of Vinson

- 2 -

(ref. 3) is extended to apply to filament reinforcements, and this analysis in turn is extended to approximate the effects of yielding of the binder surrounding the filament. The results of the analysis are used to calculate typical stresses in filaments and binders, using as a model aluminum oxide whiskers in a binder of pure aluminum.

ASSUMPTIONS

For the purpose of analysis, a single filament, binder system was postulated. The load was assumed applied at one end either to the binder alone (as if the fiber were broken within the binder), or to the fiber alone (as if the binder were cracked perpendicular to the fiber); at the other end both fiber and binder were supposed loaded so that the extension in each (at that end) was the same (see figure 1).

The analysis of this filament-binder model assuming elastic stress-strain relations is given in Appendix A. For consideration of plastic effects, the filament-binder model was considered broken up into segments and the stresses in each segment calculated by means of the elastic analysis, - with reduced values of Young's modulus used in the equations to approximate the stress-strain properties for the binder given in figure 2. The details of the procedure to take plasticity into account are given in Appendix B.

FORMULAS

The formulas, derived in Appendix A, for the stresses near the discontinuity in the model filament-binder system sketched in figure 1 are as follows:

For the shear stress between filament and binder:

$$\tau_j = \frac{\lambda}{4}\left[\frac{P_{eff}}{A_b\left(\frac{E_b}{E_f}\right)+A_f}\right]\left[\frac{\sinh\left(\lambda\frac{z}{d_f}\right)}{\cosh\left(\lambda\frac{l}{d_f}\right)}\right] \qquad (1)$$

for load applied to the binder (case a of fig. 1)

or

$$\tau_j' = -\frac{\lambda}{4}\left[\frac{P_{eff}'}{A_b\left(\frac{E_b}{E_f}\right)+A_f}\right]\left[\frac{A_b E_b}{A_f E_f}\right]\left[\frac{\sinh\left(\lambda\frac{z}{d_f}\right)}{\cosh\left(\lambda\frac{l}{d_f}\right)}\right] \qquad (2)$$

for load applied to the fiber (case b of fig. 1)

where

τ_j - shear stress in joint between filament and binder, ksi

A - cross-sectional area, in^2.

E - Young's modulus, ksi

z - distance from base (anchored) end of model, in.

d - diameter, in.

l - distance from base end of model to discontinuity, in.

P_{eff} - the effective load differential between filament and binder.

For load applied to the binder, $P_{eff} = P_b - P_f\left(\frac{A_b E_b}{A_f E_f}\right)$ (3)

For load applied to the filament, $P_{eff}' = P_f - P_b\left(\frac{A_f E_f}{A_b E_b}\right)$ (4)

P - load, kips

- 5 -

and

$$\lambda = 2\sqrt{\dfrac{2\sqrt{2}\left(\dfrac{G_f}{E_f}\right)\left[1 + \dfrac{A_f}{A_b}\left(\dfrac{E_f}{E_b}\right)\right]}{(\sqrt{2}-1) + \left(\dfrac{G_f}{G_b}\right)\left[\sqrt{\dfrac{A_b}{A_f}+2} - \sqrt{2}\right]}}$$ (5)

with

G - shear modulus of elasticity, ksi.

In these formulas, primes indicate applicability to the loading case (b) of figure 1 (load applied to the fiber), and the subscripts "f" and "b" refer to the filament and binder, respectively.

Evidently, at any station as $\mathfrak{z} = a$, for example,

$$P_{f_{@\,\mathfrak{z}=a}} = P_{f_{@\,\mathfrak{z}=\ell}} + \pi d_f \int_a^\ell \tau_j \, d\mathfrak{z}$$ (6)

The maximum shear stress occurs at $\mathfrak{z} = \ell$, so

$$\tau_{j_{max}} = \frac{\lambda}{4}\left[\frac{P_{eff}}{A_b\left(\dfrac{E_b}{E_f}\right)+A_f}\right]$$ (7)

or

$$\tau'_{j_{max}} = -\frac{\lambda}{4}\left[\frac{P_{eff}'}{A_b\left(\dfrac{E_b}{E_f}\right)+A_f}\right]\left[\frac{A_b E_b}{A_f E_f}\right]$$ (8)

In order for the fiber to pick up a given fraction ϕ of the load increment that an infinitely long fiber would pick up (as shown in Appendix C)

$$\cosh\left(\lambda\frac{\ell}{d_f}\right) = \frac{1}{1-\phi}$$ (9)

Thus the quantity λ is involved in the determination of both the maximum shear stress and the length required for filament effectiveness.

- 6 -

SAMPLE CALCULATIONS

In order to evaluate the implications of the formulas of the preceding section for properties and proportions of some interest, a series of calculations were carried out representative of aluminum oxide filaments in a binder of pure aluminum. The filament was assumed to have purely elastic stress-strain properties with a Young's modulus of 60,000 ksi and an ultimate strength of 600 ksi. The stress-strain properties of the aluminum binder were approximated by three straight lines as shown in figure 2.

Because in an actual composite the "binder" surrounding any one filament is reinforced by a host of other filaments, the calculations described in the previous paragraph represent perhaps a lower bound to the stiffnesses appropriate to the binder. In order to investigate the effect of a stiffer binder, calculations were also made for the other extreme, namely a binder having elastic properties identical to those of the filaments.

The results of these calculations are given in figures 3 - 11.

The first four of these figures show how the load is transferred from binder to filament as the distance from the discontinuity increases. With no yielding of the binder (fig. 3), the filament never does pick up much stress, because the strain in the binder is too small to stretch the filament substantially. If the binder yields, however, (fig. 4) the load is transferred to the filament in a relatively short distance, - equivalent to some 16 to 20 filament diameters even when the binder is massive

compared to the filament. The shear stresses produced near the end of the filament are the same order of magnitude as the tensile stresses applied to the binder, increasing somewhat with the increased strains produced when yielding is permitted.

The next two figures (figs. 7 and 8) show how rapidly the stress builds up in the binder when load is applied to the filament. Accompanying the rapid growth of tensile stresses in the filament are high shear stresses between filament and binder. Yielding of the binder in tension does reduce the shear stress (see figure 8), but not so much that an appreciable perturbation from the nominal load distribution for an infinite length is found anywhere beyond a distance equivalent to six or eight fiber diameters from the discontinuity. Significantly, the peak shear stress is reduced as the ratio of binder cross-sectional area to filament area is increased; simultaneously, the distance that the disturbance is propagated away from the discontinuity is increased.

The last three of these figures (figs. 9 - 11) give perhaps a more realistic picture of the nature of the stresses in an actual composite. Here the "binder" material surrounding any one filament is considered so thoroughly reinforced with other filaments that both "binder" and filament are presumed to have the same properties. Two results of the calculations based on these assumptions stand out:

(1) Even when the binder area acting with one filament is assumed to be 100 times the filament area, the stress perturbation

- 8 -

caused by a discontinuity is primarily a local one, penetrating only a few fiber diameters distant from the discontinuity.

(2) The shear stresses induced between the filament and binder at the discontinuity are very high, - for the binder/filament area ratio of 100, for example, amounting to approximately one-sixth of the applied fiber or binder stress. The magnitude of the peak shear stress is the same regardless of whether the discontinuity is of the nature of a broken filament or a crack in the binder perpendicular to the filament.

DISCUSSION

While the formulas, calculations, and plots so far presented may help to shed some light on the mechanics of filamentary reinforcement, they leave two pertinent questions substantially unanswered. These questions are:

(1) Why does Parratt (ref. 2) arrive at a length of filament needed which is so much greater than would appear from the results so far shown herein?

(2) What does this analysis reveal which may be helpful in furthering the development of filamentary composites?

This discussion will be concerned primarily with the answers to these questions.

Filament length required for effectiveness. - Equations (7) and (9) show that the filament length required for effectiveness and also the maximum shear stress between filament and binder depend upon the parameter λ . The dependence is direct and linear in the case of the maximum shear stress, and evidently, rewriting (9)

$$\frac{\ell}{d_f} = \frac{\cosh^{-1}\left(\frac{1}{1-\phi}\right)}{\lambda} \tag{10}$$

inverse and linear in the case of the length required. Thus a reduction in shear stress via a reduction in λ should be expected to be accompanied by an increase in the filament length needed for effectiveness.

- 10 -

As has been shown (fig. 11) the shear stresses for the most realistic

model considered are very high, so high that in practice they most probably

will not be achieved. Rather yielding in shear will occur to relieve the

peak bond stresses. This yielding is comparable to a reduction in G_b ,

hence (see equation (5)) to a reduction in λ , and hence to an increase

in the filament length required for effectiveness.

Because the parameter λ has so much bearing upon the mechanics of

reinforcement, calculations were made to determine the sensitivity of the

value of λ to changes in the various quantities of which it is comprised.

Thus, as shown in figures 12, λ is insensitive to variations in the ratio of

E_f to E_b , somewhat more sensitive to variations in the ratio of G_f to G_b ,

and most sensitive to the area ratio A_f to A_b . Inasmuch as failure of the

bond between binder and filament may reduce the effective value of G_b to

zero, however, evidently λ may in practice become very small and hence

the filament lengths required for effectiveness may indeed approach the

values suggested in reference 2.

Implications for further developments. - The facts that the shear stresses

between filament and binder are high near a discontinuity, and that (unless

alleviated by yielding in shear) they are not propagated far from the dis-

continuity, combine to make the attainment of a satisfactory bond between

filament and binder a critical problem. In the elastic case, in just the

same way that a relatively short fiber can act as effectively as a long

filament (provided the bond is adequate), fracture of the bond near the

discontinuity in a long filament will not be reduced, by the decreasing length of filament acting, until the bond fracture has been propagated along the major portion of the filament. Thus, some sort of resilient bond is essential to prevent a major loss in filament effectiveness from discontinuities, unless very strong bonding is assured.

CONCLUDING REMARKS

Formulas derived for the local stresses near a discontinuity in filament-reinforced, composite materials show that a parameter λ,- comprising the relative stiffnesses and cross-sectional areas of filament and associated binder as defined herein, to a large extent governs both the degree to which the stresses are concentrated near the discontinuity, and the magnitude of the peak shear stresses induced in the bond between filament and binder. In general the peak bond stresses are shown to be high, so high that unless reduced by a non-destructuve yielding in shear they may well limit the attainment of the potentials available with high strength filaments.

APPENDIX A. - DERIVATION OF EQUATIONS

The derivation of the equations given in the main text of this paper for the stresses near a discontinuity in a filament-reinforced, composite material follows closely the procedure of reference 3. Because that reference may not be readily available, and because there are necessarily minor differences from the procedures given there, a reasonably complete derivation is given here, as follows.

Consider an element of the composite consisting of one filament of length $2l$ and diameter d_f, and associated binder, - of somewhat greater length, - assumed to surround the fiber as a concentric circular cylinder of diameter D_b. Assume a total tensile load P_b applied uniformly to both ends of the binder. Suppose z- and r-axes with origins at the midpoint along the length and at the center of the fiber cross-section, respectively.

With the foregoing model, and the assumption that straight lines in the cross-sections of filament and binder remain straight after deformation, the following equations may be written:

For equilibrium

$$\tau_j = \frac{1}{\pi d_f}\left(\frac{dF_b}{dz}\right) \tag{A-1}$$

and

$$\tau_j = -\frac{1}{\pi d_f}\left(\frac{dF_f}{dz}\right) \tag{A-2}$$

where

      F - force acting in filament or binder (a function of z).

- 13 -

Strain-displacement relations

$$\epsilon_{b_z} = \frac{dU_{b_z}}{dz} \qquad\qquad \epsilon_{f_z} = \frac{dU_{f_z}}{dz} \qquad (A-3)$$

$$\epsilon_{b_r} = \frac{dU_{b_r}}{dr} \qquad\qquad \epsilon_{f_r} = \frac{dU_{f_r}}{dr} \qquad (A-4)$$

where

     U - displacement

     ϵ - strain

And the stress-displacement relations, at $z = 0$

$$\frac{dU_{F_b}}{dz} = \frac{F_b}{A_b E_b} \qquad (A-5)$$

$$\frac{dU_{\bar{r}_f}}{dz} = \frac{F_f}{A_f E_f} \qquad (A-6)$$

with the subscript $\bar{F}$ used to designate the centroidal location.

Because of the assumption that straight lines in each material remain straight, the shear strain γ may be expressed

$$\gamma_b = -\left[\frac{U_j - U_{\bar{r}_b}}{\bar{r}_b}\right] = \frac{\tau_j}{G_b} \qquad (A-7)$$

and

$$\gamma_f = -\left[\frac{U_{\bar{r}_f} - U_j}{\bar{r}_f}\right] = \frac{\tau_j}{G_f} \qquad (A-8)$$

where $\bar{r}$ is the radial distance from the origin to the center of gravity

of the material cross-section, i.e.

$$\bar{r}_b = \sqrt{\frac{D_b^2 + d_f^2}{8}} - \frac{d_f}{2} \qquad (A-9)$$

- 14 -

$$\bar{r}_f = \frac{d_f}{2} - \sqrt{\frac{d_f^2}{8}} \tag{A-10}$$

Equating the γ_j's and U_j's in (A-7) and (A-8) and solving for U_j

$$U_j = \frac{\dfrac{G_f}{\bar{r}_f} U_{\bar{r}_f} + \dfrac{G_b}{\bar{r}_b} U_{\bar{r}_b}}{\dfrac{G_f}{\bar{r}_f} + \dfrac{G_b}{\bar{r}_b}} \tag{A-11}$$

Differentiating (A-5) and (A-6)

$$\frac{dF_b}{dz} = A_b E_b U_{\bar{r}_b}'' \tag{A-12}$$

$$\frac{dF_f}{dz} = A_f E_f U_{\bar{r}_f}'' \tag{A-13}$$

Substituting (A-12) and (A-13) in (A-1) and (A-2)

$$\gamma_j = \frac{1}{\pi d_f} A_b E_b U_{\bar{r}_b}'' \tag{A-14}$$

or

$$\gamma_j = -\frac{1}{\pi d_f} A_f E_f U_{\bar{r}_f}'' \tag{A-15}$$

And substituting (A-14) and (A-15) into (A-7) and (A-8)

$$-G_b \left[\frac{U_j - U_{\bar{r}_b}}{\bar{r}_b} \right] = \frac{1}{\pi d_f} A_b E_b U_{\bar{r}_b}'' \tag{A-16}$$

$$-G_f \left[\frac{U_{\bar{r}_f} - U_j}{\bar{r}_f} \right] = -\frac{1}{\pi d_f} A_f E_f U_{\bar{r}_f}'' \tag{A-17}$$

From (A-16)

$$U_{\bar{r}_b}'' + \frac{\pi d_f G_b}{A_b E_b \bar{r}_b} \left(U_j - U_{\bar{r}_b} \right) = 0 \tag{A-18}$$

- 15 -

and from (A-17)

$$-U_{\bar{r}_f}'' + \frac{\pi d_f \, G_f}{A_f E_f \bar{r}_f}\left(U_{\bar{r}_f} - U_j\right) = 0 \tag{A-19}$$

Substituting (A-11) in (A-18) and simplifying

$$-U_{\bar{r}_b}'' + \frac{\pi d_f}{A_b E_b}\left[\frac{\frac{G_b}{\bar{r}_b}\frac{G_f}{\bar{r}_f}}{\frac{G_b}{\bar{r}_b} + \frac{G_f}{\bar{r}_f}}\right]\left(U_{\bar{r}_b} - U_{\bar{r}_f}\right) = 0 \tag{A-20}$$

Similarly

$$U_{\bar{r}_f}'' + \frac{\pi d_f}{A_f E_f}\left[\frac{\frac{G_b}{\bar{r}_b}\frac{G_f}{\bar{r}_f}}{\frac{G_b}{\bar{r}_b} + \frac{G_f}{\bar{r}_f}}\right]\left(U_{\bar{r}_b} - U_{\bar{r}_f}\right) = 0 \tag{A-21}$$

Adding (A-20) and (A-21)

$$\left(U_{\bar{r}_b}'' - U_{\bar{r}_f}''\right) - K^2\left(U_{\bar{r}_b} - U_{\bar{r}_f}\right) = 0 \tag{A-22}$$

where

$$K^2 = \pi d_f\left[\frac{\frac{G_b}{\bar{r}_b}\frac{G_f}{\bar{r}_f}}{\frac{G_b}{\bar{r}_b} + \frac{G_f}{\bar{r}_f}}\right]\left(\frac{1}{A_b E_b} + \frac{1}{A_f E_f}\right) \tag{A-23}$$

Solving (A-22)

$$U_{\bar{r}_b} - U_{\bar{r}_f} = N \cosh K_3 + M \sinh K_3 \tag{A-24}$$

The appropriate boundary conditions are

$$3 = 0, \qquad U_{\bar{r}_{b_o}} = U_{\bar{r}_{f_o}} = 0 \tag{A-25}$$

and

$$3 = \ell, \qquad \begin{cases} U_{\bar{r}_{b_I}}' = \dfrac{P_b}{A_b E_b} \\[2mm] U_{\bar{r}_{f_I}} = 0 \end{cases} \tag{A-26}$$

- 16 -

Hence

$$N = 0 \tag{A-27}$$

$$M = \frac{P_b}{A_b\,E_b\,K\cosh Kl} \tag{A-28}$$

Substituting (A-27) and (A-28) in (A-24)

$$U_{\bar{r}_b} - U_{\bar{r}_f} = \frac{P_b}{A_b\,E_b\,K\cosh Kl}\ \sinh K\gamma \tag{A-29}$$

Substituting (A-29) in (A-20)

$$U_{\bar{r}_b}'' = \frac{\pi d_f}{A_b\,E_b}\left[\frac{\dfrac{G_b}{\bar{r}_b}\dfrac{G_f}{\bar{r}_f}}{\dfrac{G_b}{\bar{r}_b}+\dfrac{G_f}{\bar{r}_f}}\right]\left(\frac{P_b\ \sinh K\gamma}{A_b\,E_b\,K\cosh Kl}\right) \tag{A-30}$$

Integrating

$$U_{\bar{r}_b}' = \frac{\pi d_f}{A_b\,E_b}\left[\frac{\dfrac{G_b}{\bar{r}_b}\dfrac{G_f}{\bar{r}_f}}{\dfrac{G_b}{\bar{r}_b}+\dfrac{G_f}{\bar{r}_f}}\right]\left(\frac{P_b\ \cosh K\gamma}{A_b\,E_b\,K^2\cosh Kl}\right) + Q \tag{A-31}$$

Substituting from (A-26) and simplifying

$$Q = \frac{P_b}{A_b\,E_b + A_f\,E_f} \tag{A-32}$$

Putting this back in (A-31) and integrating again

$$U_{\bar{r}_b} = \frac{\pi d_f}{A_b\,E_b}\left[\frac{\dfrac{G_b}{\bar{r}_b}\dfrac{G_f}{\bar{r}_f}}{\dfrac{G_b}{\bar{r}_b}+\dfrac{G_f}{\bar{r}_f}}\right]\left(\frac{P_b\ \sinh K\gamma}{A_b\,E_b\,K^3\cosh Kl}\right) + Q\gamma + R \tag{A-33}$$

Clearly, from (A-25)

$$R = 0 \tag{A-34}$$

- 17 -

Hence

$$U_{\bar{r}_b} = \frac{P_b}{A_b E_b + A_f E_f}\left[\, \mathcal{Z} \, + \frac{A_f E_f}{A_b E_b}\left(\frac{\sinh K_{\mathcal{Z}}}{K\cosh K\ell}\right)\right] \tag{A-35}$$

Similarly it can be shown that

$$U_{\bar{r}_f} = \frac{P_b}{A_b E_b + A_f E_f}\left[\, \mathcal{Z} \, - \frac{\sinh K_{\mathcal{Z}}}{K\cosh K\ell}\right] \tag{A-36}$$

Substituting (A-35) and (A-36) in (A-11)

$$U_j = \frac{P_b}{A_b E_b + A_f E_f}\left[\mathcal{Z} + \left\{\frac{\frac{G_b}{\bar{r}_b}\left(\frac{A_f E_f}{A_b E_b}\right) - \frac{G_f}{\bar{r}_f}}{\frac{G_b}{\bar{r}_b} + \frac{G_f}{\bar{r}_f}}\right\}\left(\frac{\sinh K_{\mathcal{Z}}}{K\cosh K\ell}\right)\right] \tag{A-37}$$

Also, substituting (A-29) in (A-21)

$$U_{\bar{r}_f}'' = \frac{-\pi d_f}{A_f E_f}\left[\frac{\frac{G_b}{\bar{r}_b}\frac{G_f}{\bar{r}_f}}{\frac{G_b}{\bar{r}_b} + \frac{G_f}{\bar{r}_f}}\right]\left(\frac{P_b}{A_b E_b}\right)\left(\frac{\sinh K_{\mathcal{Z}}}{K\cosh K\ell}\right) \tag{A-38}$$

Which, substituted in (A-15) yields

$$\tau_j = \frac{P_b}{A_b E_b}\left[\frac{\frac{G_b}{\bar{r}_b}\frac{G_f}{\bar{r}_f}}{\frac{G_b}{\bar{r}_b} + \frac{G_f}{\bar{r}_f}}\right]\left(\frac{\sinh K_{\mathcal{Z}}}{K\cosh K\ell}\right) \tag{A-39}$$

Let us now write

$$\lambda = K d_f = 2\sqrt{\frac{2\sqrt{2}\left(\frac{G_f}{E_f}\right)\left[1 + \frac{A_f}{A_b}\left(\frac{E_f}{E_b}\right)\right]}{(\sqrt{2}-1) + \left(\frac{G_f}{G_b}\right)\left[\sqrt{\frac{A_b}{A_f}+2} - \sqrt{2}\right]}} \tag{A-40}$$

Substituting (A-40) in (A-39) yields, after some manipulation

$$\tau_j = \frac{\lambda}{4}\left[\frac{P_b}{A_b\left(\frac{E_b}{E_f}\right)+A_f}\right]\left(\frac{\sinh\left(\lambda\frac{\mathcal{Z}}{d_f}\right)}{\cosh\left(\lambda\frac{\ell}{d_f}\right)}\right) \tag{A-41}$$

- 18 -

The derivation of the parallel case for load applied to the filament instead
of the binder is identical except that the boundary conditions employed
instead of those given by equation (A-26) are

$$
z = \ell , \qquad \left\{ \begin{array}{l} U'_{F_{b_1}} = 0 \\[2mm] U'_{F_{f_1}} = \dfrac{P_f}{A_f E_f} \end{array} \right.
\qquad\qquad (A\text{-}42)
$$

And, using these we find

$$
\tau'_j = - \frac{\lambda}{4}\left[\frac{P_f}{A_b\left(\dfrac{E_b}{E_f}\right)+A_f}\right]\left(\frac{\sinh\left(\lambda\,\dfrac{z}{d_f}\right)}{\cosh\left(\lambda\,\dfrac{z}{d_f}\right)}\right)\left(\frac{A_b E_b}{A_f E_f}\right)
\qquad (A\text{-}43)
$$

If load is applied to both filament and binder, the same equations (A-41) or
(A-43) may be applied by subtracting from the applied load the part of the
load which produces simply an equal, uniform extension of both filament
and binder. The remainder of the load P_{eff} or P'_{eff} is then assumed applied
entirely to binder or filament depending upon which of the two carries the
greater load, thus:

For the greater load on the binder

$$
P_{eff} = P_b - P_f\left(\frac{A_b E_b}{A_f E_f}\right)
\qquad\qquad (A\text{-}44)
$$

And for the greater load on the filament

$$
P'_{eff} = P_f - P_b\left(\frac{A_f E_f}{A_b E_b}\right)
\qquad\qquad (A\text{-}45)
$$

Inspection of equations (A-41) and (A-43) reveals that τ_j is a maximum

when $z = \ell$.   Hence

$$
\tau_{j_{max}} = \frac{\lambda}{4}\left[\frac{P_{eff}}{A_b\left(\dfrac{E_b}{E_f}\right)+A_f}\right]
\qquad\qquad (A\text{-}46)
$$

$$
\tau'_{j_{max}} = - \frac{\lambda}{4}\left[\frac{P'_{eff}}{A_b\left(\dfrac{E_b}{E_f}\right)+A_f}\right]\left(\frac{A_b E_b}{A_f E_f}\right)
\qquad\qquad (A\text{-}47)
$$

- 19 -

APPENDIX B. - APPROXIMATE PROCEDURE USED TO TAKE
PLASTICITY INTO ACCOUNT

In order to take into account yielding of the binder material, a number
of simplifying assumptions were employed. The material stress-strain
curve was linearized into that shown in figure 2, - the discontinuities used
result in four stress ranges for each of which the secant modulus of
elasticity is equal to the tangent modulus of elasticity. The filament-binder
model under consideration was broken up into segments within which the
stress varied over the ranges corresponding to those of figure 2; each
segment was then analyzed as if it were part of an elastic continuum having
properties as given by figure 2 for the proper stress range, and the segment
lengths required to match the chosen end stresses were calculated from the
elastic equations as given in the text of this paper. In all cases the ratio of
shear modulus to Young's modulus for the binder material was assumed
constant at a value of 0.385.

The procedure used for the analysis of inelastic effects is perhaps best
illustrated by an example. Let us consider the case of an aluminum oxide
filament of unit area surrounded by aluminum binder of equal area. Suppose
a load corresponding to 600 ksi applied to the filament (case (b) of fig. 1),
and stress-strain properties for the binder as in figure 2. Let us determine
the filament length required for the binder to pick up 97% of the load that it
would if the filament-binder model were infinitely long.

- 20 -

We have

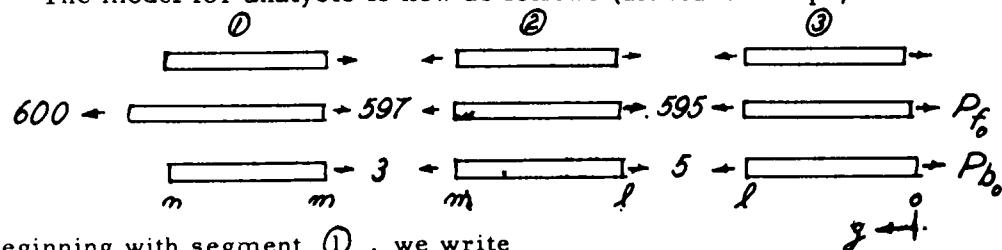$$E_f = 60,000 \text{ ksi}$$

$$A_f = 1 \text{ in.}^2$$

$$G_f/E_f = 0.385$$

$$E_b \quad \text{from figure 2}$$

$$A_b = 1 \text{ in.}^2$$

$$G_b/E_b = 0.385$$

The model for analysis is now as follows (all loads in kips)

Beginning with segment ① , we write

$$3 = \pi d_f \int_m^m \tau_j' \, dz \tag{B-1}$$

From equation (2)

$$\tau_{j_0}' = -\frac{\lambda_0}{4}\left[\frac{600}{1\left(\frac{10,000}{60,000}\right)+1}\right]\left[\frac{1(10,000)}{1(60,000)}\right]\left[\frac{\sinh\left(\lambda_0 \frac{z}{d_f}\right)}{\cosh\left(\lambda_0 \frac{m}{d_f}\right)}\right] \tag{B-2}$$

With

$$\lambda_0 = 2\sqrt{\frac{2\sqrt{2}\,(0.385)\left[1+1\left(\frac{60,000}{10,000}\right)\right]}{(\sqrt{2}-1)+\left[\frac{0.385(60,000)}{0.385(10,000)}\right]\left[\sqrt{1+2}-\sqrt{2}\right]}}$$

$$= 3.62 \tag{B-3}$$

And $d_f = \sqrt{\dfrac{4}{\pi}} = 1.128$, so

$$\gamma_j' = -77.6\left[\frac{\sinh\left(\frac{3.62}{1.128}\,z\right)}{\cosh(3.21\,m)}\right] \tag{B-4}$$

Substituting in (B-1)

$$\frac{3}{1.128\,\pi} = -\frac{77.6}{\cosh(3.21m)}\int_m^m \sinh(3.21\,z)\,dz \tag{B-5}$$

Or

$$0.0109 = -\frac{1}{3.21\cosh(3.21m)}\left[\cosh(3.21m) - \cosh(3.21m)\right] \tag{B-6}$$

$$0.035 = 1 - \frac{\cosh(3.21m)}{\cosh(3.21m)} \tag{B-7}$$

And

$$\frac{\cosh(3.21m)}{\cosh(3.21m)} = 0.965 \tag{B-8}$$

Similarly, for segment ②

$$5 = 3 + \pi d_f \int_m^\ell \gamma_j'\,dz \tag{B-9}$$

Now

$$\gamma_{j_②}' = -\frac{\lambda_②}{4}\left[\frac{P_{eff}'}{1\left(\frac{2000}{60,000}\right)+1}\right]\left[\frac{1(2000)}{1(60,000)}\right]\left[\frac{\sinh\left(\lambda_②\frac{z}{d_f}\right)}{\cosh\left(\lambda_②\frac{m}{d_f}\right)}\right] \tag{B-10}$$

With, from equation (4)

$$P_{eff}' = 597 - 3\left(\frac{60,000}{2000}\right) = 507 \ kips \tag{B-11}$$

And

$$\lambda_② = 3.69 \tag{B-12}$$

- 22 -

Substituting in (B-9) and integrating as before, we find

$$\frac{\cosh(3.69\,\ell)}{\cosh(3.69\,m)} = 0.878 \tag{B-13}$$

The length ℓ depends upon the percent effectiveness desired,

for $\phi = 0.97$, from equation (10)

$$\frac{\ell}{d_f} = \frac{\cosh^{-1}(33.33)}{\lambda_{\textcircled{9}}} \tag{B-14}$$

where

$$\lambda_{\textcircled{9}} = 3.70 \tag{B-15}$$

for $E_b = 500$ ksi. Putting (B-15) in (B-14)

$$\frac{\ell}{d_f} = 1.134 \tag{B-16}$$

This may now be substituted in (B-13) to find

$$\frac{m}{d_f} = 1.169 \tag{B-17}$$

And in (B-8) to find

$$\frac{m}{d_f} = 1.180 \tag{B-18}$$

With these lengths established, the various formulas may be readily

applied to determine shear or axial stresses.

APPENDIX C. - DETERMINATION OF LENGTH REQUIRED FOR A GIVEN EFFECTIVENESS

The length-effectiveness relation will be derived only for case (a) of figure 1 (load applied to binder). The derivation for case (b) would be similar.

Let us define the effectiveness fraction ϕ as follows:

$$\phi = \frac{P_{f_{eff}} - P_{f_{applied}}}{P_{f_{\infty}} - P_{f_{applied}}} \tag{C-1}$$

where

$P_{f_{eff}}$ - load carried at midpoint of actual filament of length 2ℓ

$P_{f_{applied}}$ - load applied to end of filament

$P_{f_{\infty}}$ - load that would be carried at midpoint of infinitely long filament.

Now

$$P_{f_{eff}} = P_{f_{applied}} + \pi d_f \int_0^\ell \tau_j \, dz \tag{C-2}$$

With

$$\tau_j = \frac{\lambda}{4} \left[\frac{P_b - P_{f_{applied}} \left(\frac{A_b E_b}{A_f E_f} \right)}{A_b \left(\frac{E_b}{E_f} \right) + A_f} \right] \left[\frac{\sinh\left(\lambda \frac{z}{d_f} \right)}{\cosh\left(\lambda \frac{\ell}{d_f} \right)} \right] \tag{C-3}$$

Substituting (C-3) in (C-2) and integrating

$$P_{f_{eff}} = P_{f_{applied}} + \left[\frac{\frac{P_b}{A_b E_b} - \frac{P_{f_{applied}}}{A_f E_f}}{\frac{1}{A_b E_b} + \frac{1}{A_f E_f}}\right]\left[1 - \frac{1}{\cosh\left(\lambda \frac{\ell}{d_f}\right)}\right] \qquad (C-4)$$

since $\pi \frac{d_f^2}{4} = A_f$. Solving for $\cosh\left(\lambda \frac{\ell}{d_f}\right)$ gives

$$\cosh\left(\lambda \frac{\ell}{d_f}\right) = \frac{\frac{P_b}{A_b E_b} - \frac{P_{f_{applied}}}{A_f E_f}}{\frac{P_b + P_{f_{applied}}}{A_b E_b} - P_{f_{eff}}\left[\frac{1}{A_b E_b} + \frac{1}{A_f E_f}\right]} \qquad (C-5)$$

or

$$\cosh\left(\lambda \frac{\ell}{d_f}\right) = \frac{P_{eff}}{P - P_{f_{eff}}\left(1 + \frac{A_b E_b}{A_f E_f}\right)} \qquad (C-6)$$

Noting tnat

$$P_{eff} = P - P_{f_{applied}}\left(1 + \frac{A_b E_b}{A_f E_f}\right) \qquad (C-7)$$

And

$$P = P_{f_\infty}\left(1 + \frac{A_b E_b}{A_f E_f}\right) \qquad (C-8)$$

This becomes

$$\cosh\left(\lambda \frac{\ell}{d_f}\right) = \frac{P_{f_\infty} - P_{f_{applied}}}{P_{f_\infty} - P_{f_{eff}}} \qquad (C-9)$$

Which is equivalent to

$$\cosh\left(\lambda \frac{\ell}{d_f}\right) = \frac{1}{1 - \phi} \qquad (C-10)$$

APPENDIX D. - LIST OF SYMBOLS

For convenience, the symbols used are tabulated and defined below: -

A	cross-sectional area
D	diameter
E	Young's modulus
F	force
G	shear modulus of elasticity
K	a parameter defined in Appendix A
M, N, Q, R	constants of integration
P	load
U	displacement
a	distance along filament
d	diameter
l, m, n	distances along filament
r	radial distance from center of filament
x	distance from discontinuity in filament or binder
z	distance from mid-point of filament
γ	shear strain
ϵ	longitudinal strain
λ	a parameter defined by equation (5)
τ	shear stress
ϕ	effectiveness parameter, defined in Appendix C

- 26 -

Subscripts

b binder

f filament

j joint

o origin

∞ denotes application to filament of infinite length

$applied$ applied

eff effective

max maximum

Superscripts

bar   centroidal

primes   denote application to case (b) of figure 1, or differentiation

REFERENCES

1. Jech, R. W.; McDanels, D. L.; and Weeton, J. W.: Fiber

    Reinforced Metallic Composites. Proceedings of 6th Sagamore

    Ord. Materials Res. Conf., Racquette Lake, N. Y., Aug. 1959.

2. Parratt, N. J.: Defects in Glass Fibers and Their Effect on the

    Strength of Plastic Mouldings. Rubber and Plastics Age, Vol. 41,

    No. 3, 1960.

3. Vinson, Jack R.: An Investigation of the Behavior of Brittle

    Coatings on Beams in Tension. General Electric Co., Space

    Sciences Laboratory, Applied Mechanics Memorandum #48,

    April 8, 1958.

MODELS USED FOR ANALYSIS
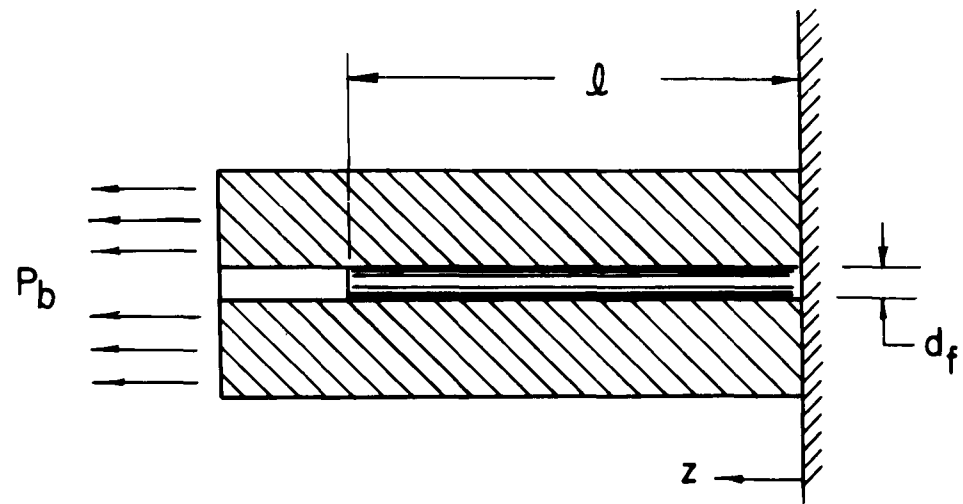
CASE (a) — LOAD APPLIED
TO BINDER
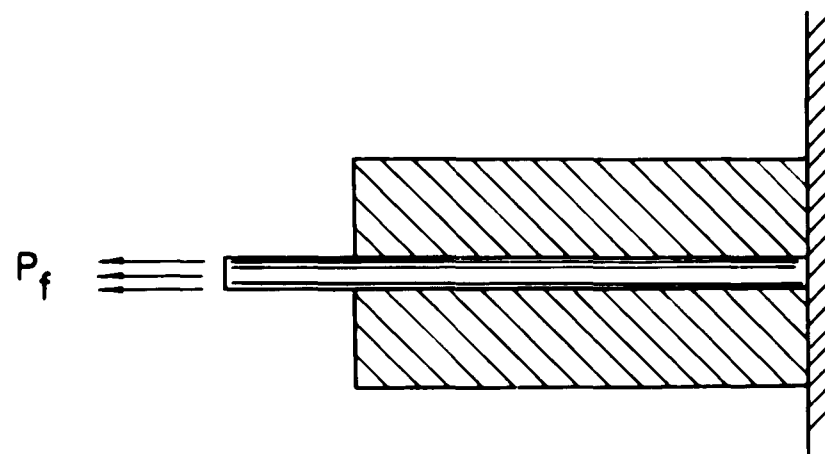
CASE (b) — LOAD APPLIED
TO FIBER

Figure 1

APPROXIMATE STRESS-STRAIN PROPERTIES
USED TO CHARACTERIZE ALUMINUM BINDER
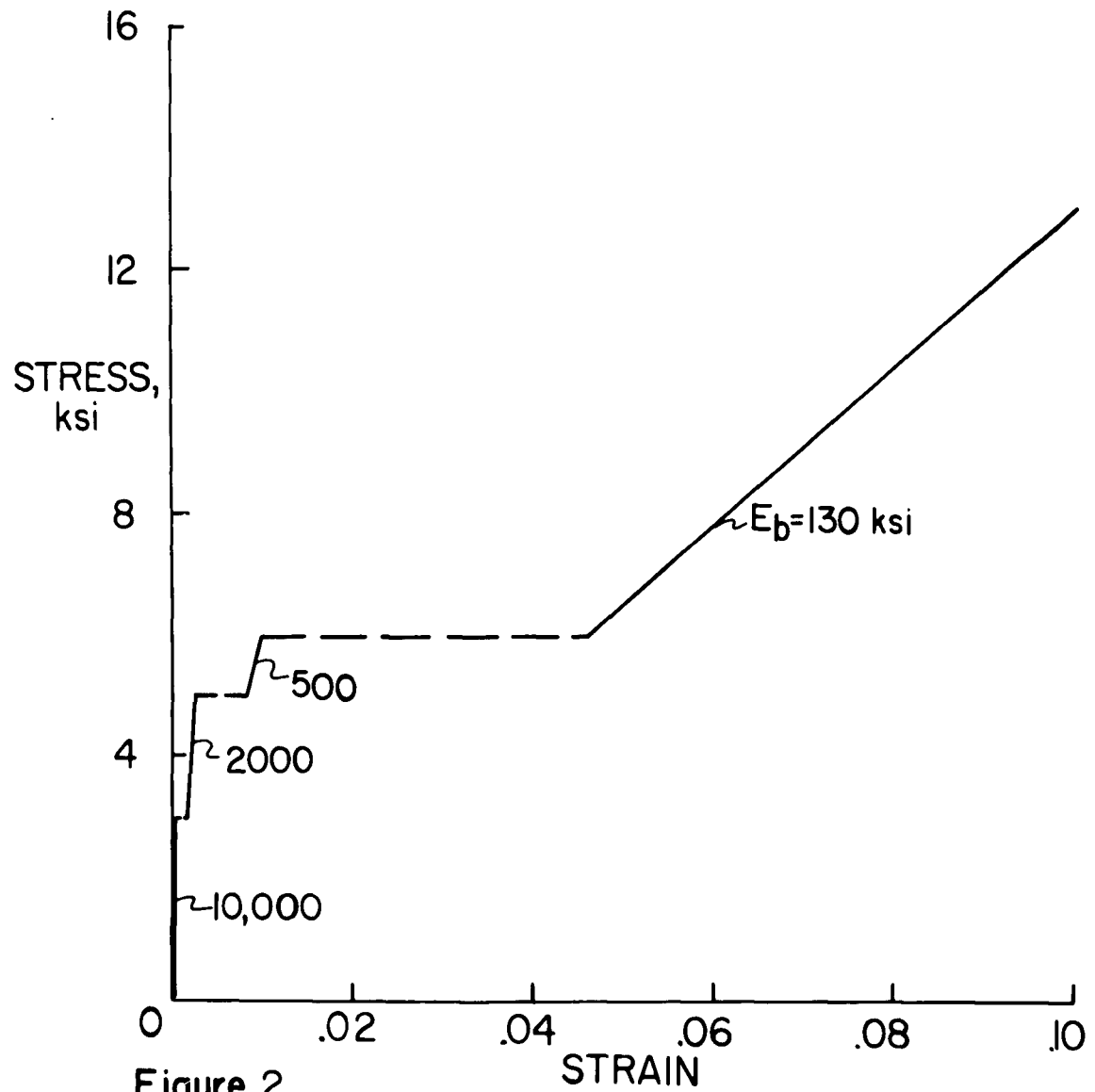
Figure 2

CALCULATED TENSILE STRESSES σ_f INDUCED IN Al_2O_3 FILAMENT BY TENSION APPLIED TO AN ELASTIC, Al BINDER.
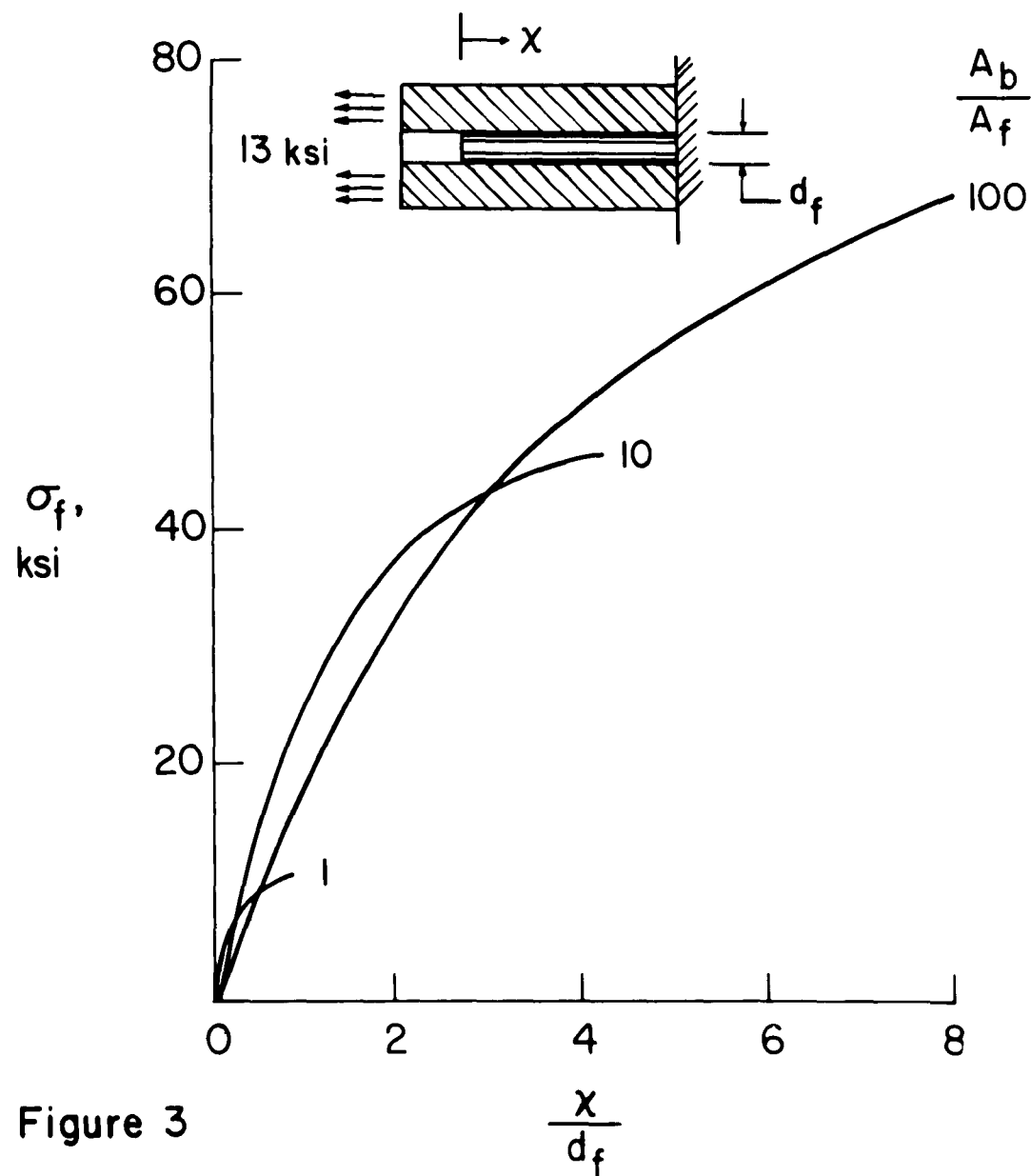
Figure 3

CALCULATED TENSILE STRESSES σ_f INDUCED IN Al_2O_3 FILAMENT BY TENSION APPLIED TO AN INELASTIC Al BINDER. (BINDER PROPERTIES AS IN FIG. 2 WITH $G_b/E_b = 0.385$)
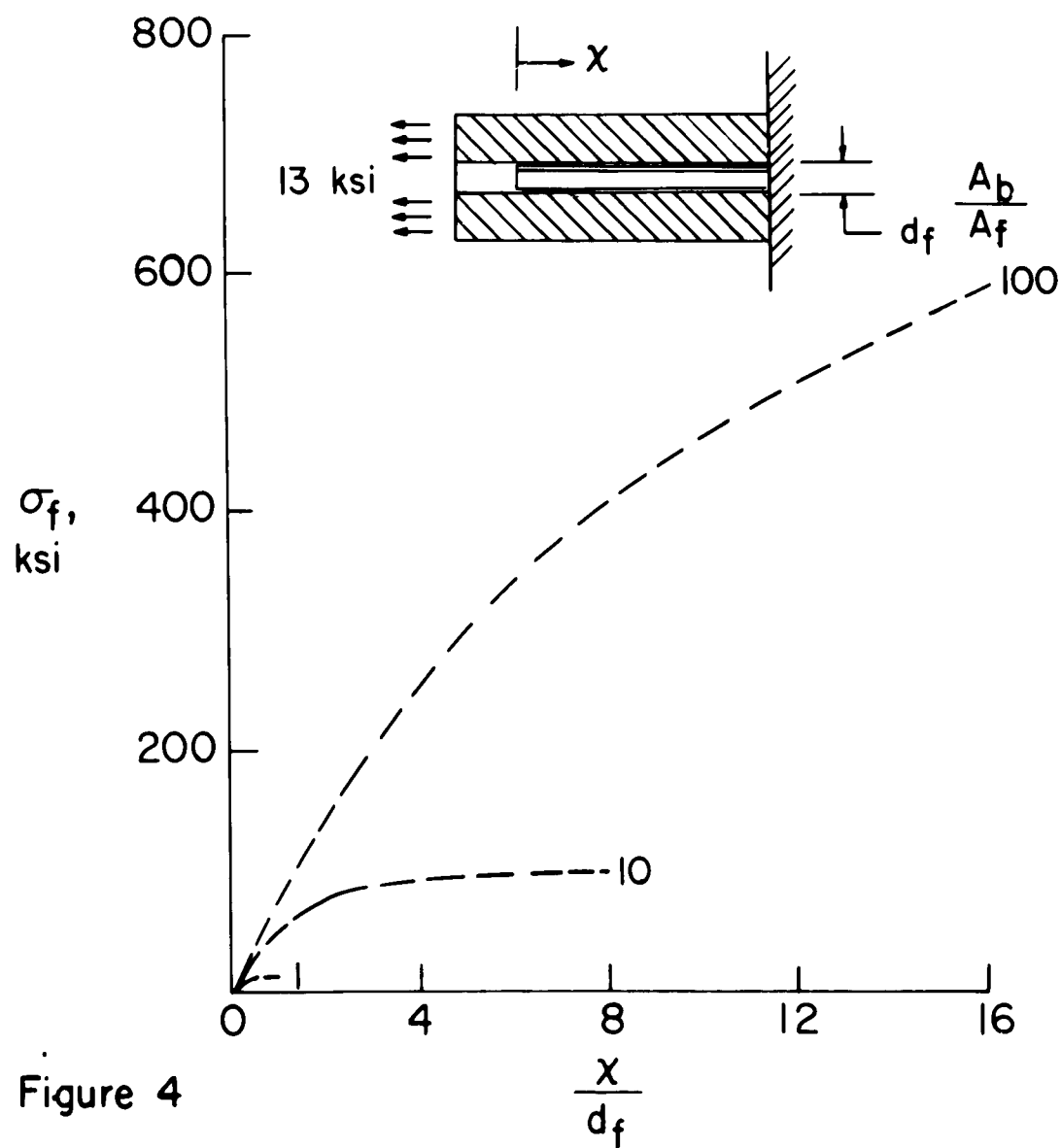

Figure 4

CALCULATED ELASTIC SHEAR STRESSES τ_j INDUCED BETWEEN $Al_2 O_3$ FILAMENT AND Al BINDER BY TENSION APPLIED TO BINDER
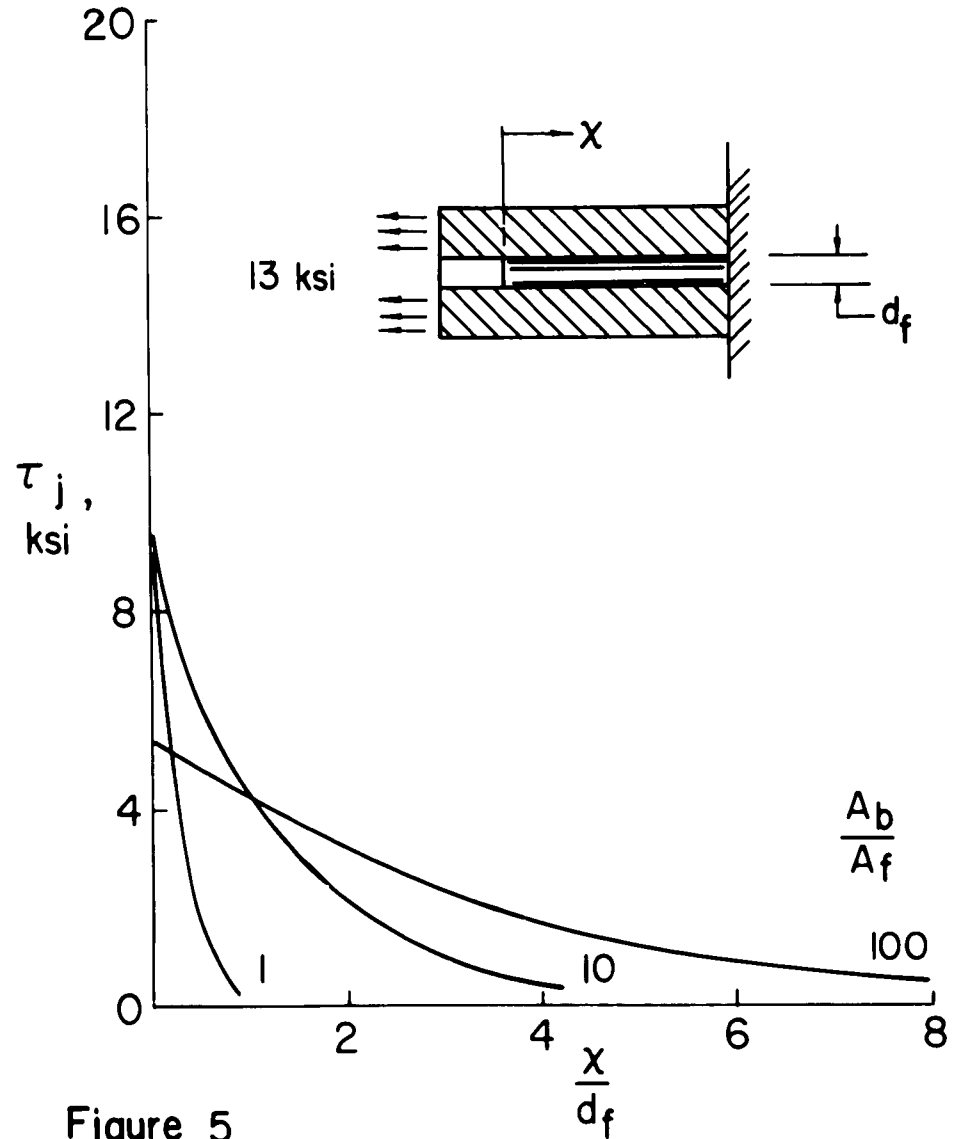
Figure 5

CALCULATED SHEAR STRESSES τ_j INDUCED BETWEEN Al_2O_3 FILAMENT AND INELASTIC Al BINDER BY TENSION APPLIED TO BINDER. (BINDER PROPERTIES AS IN FIG. 2 WITH $^{G}b/_{E_b} = 0.385$)
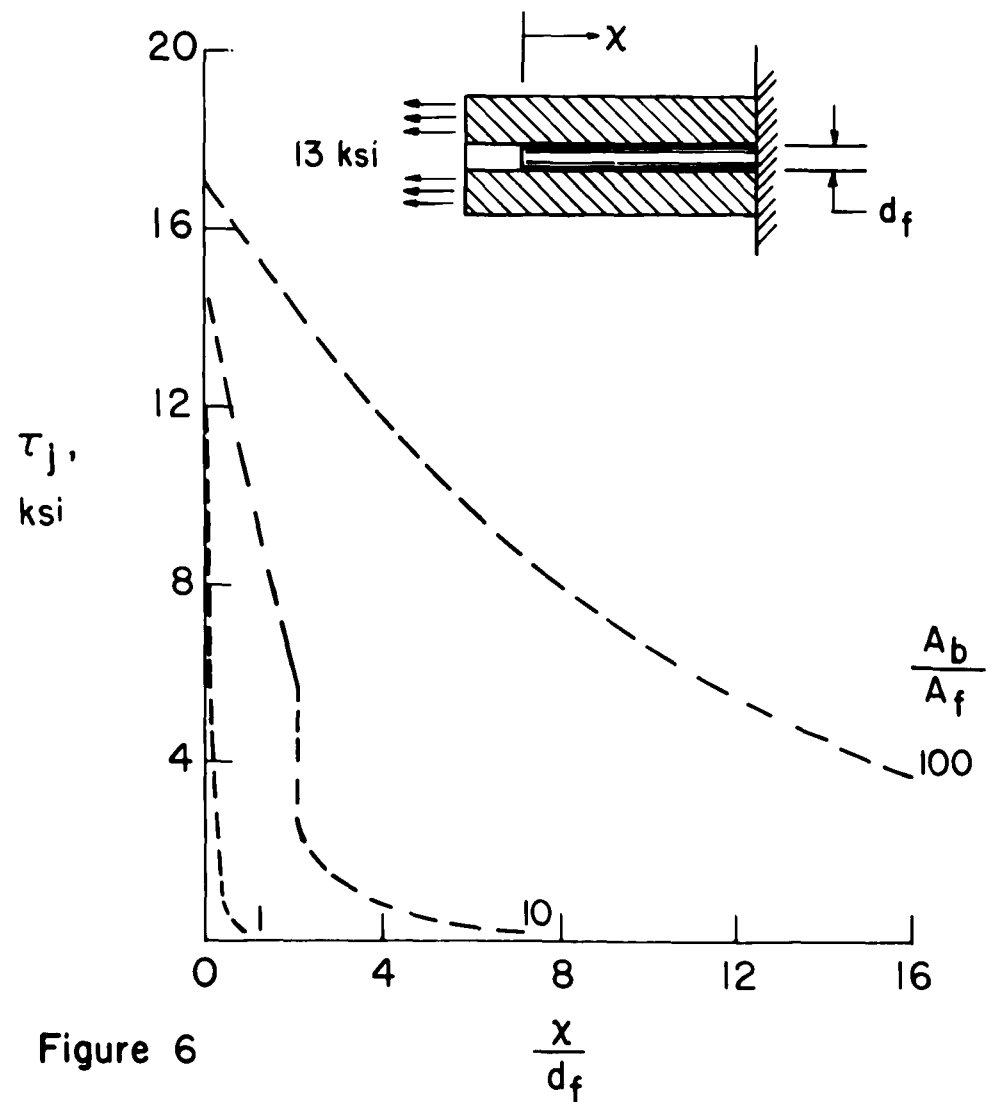
Figure 6

CALCULATED STRESSES σ_b INDUCED IN Al BINDER BY TENSION APPLIED TO Al_2O_3 FILAMENT.(BINDER ELASTIC, OR HAVING PROPEPTIES AS IN FIGURE 2 WITH $G_{b/E_b} = 0.385$)
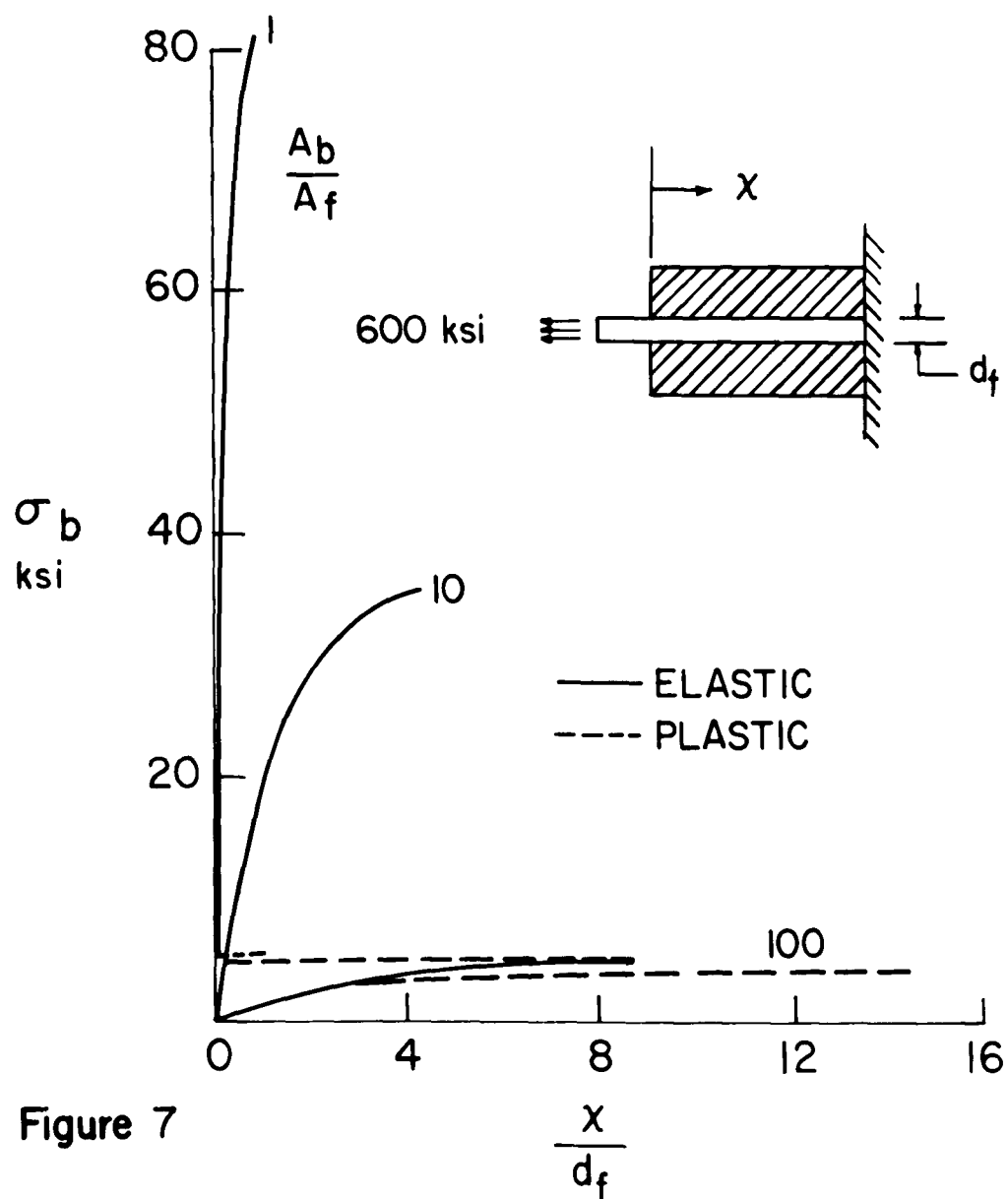
Figure 7

CALCULATED SHEAR STRESSES τ_j
BETWEEN FILAMENT AND BINDER OF AN
Al-Al$_2$O$_3$ COMPOSITE INDUCED BY TENSION
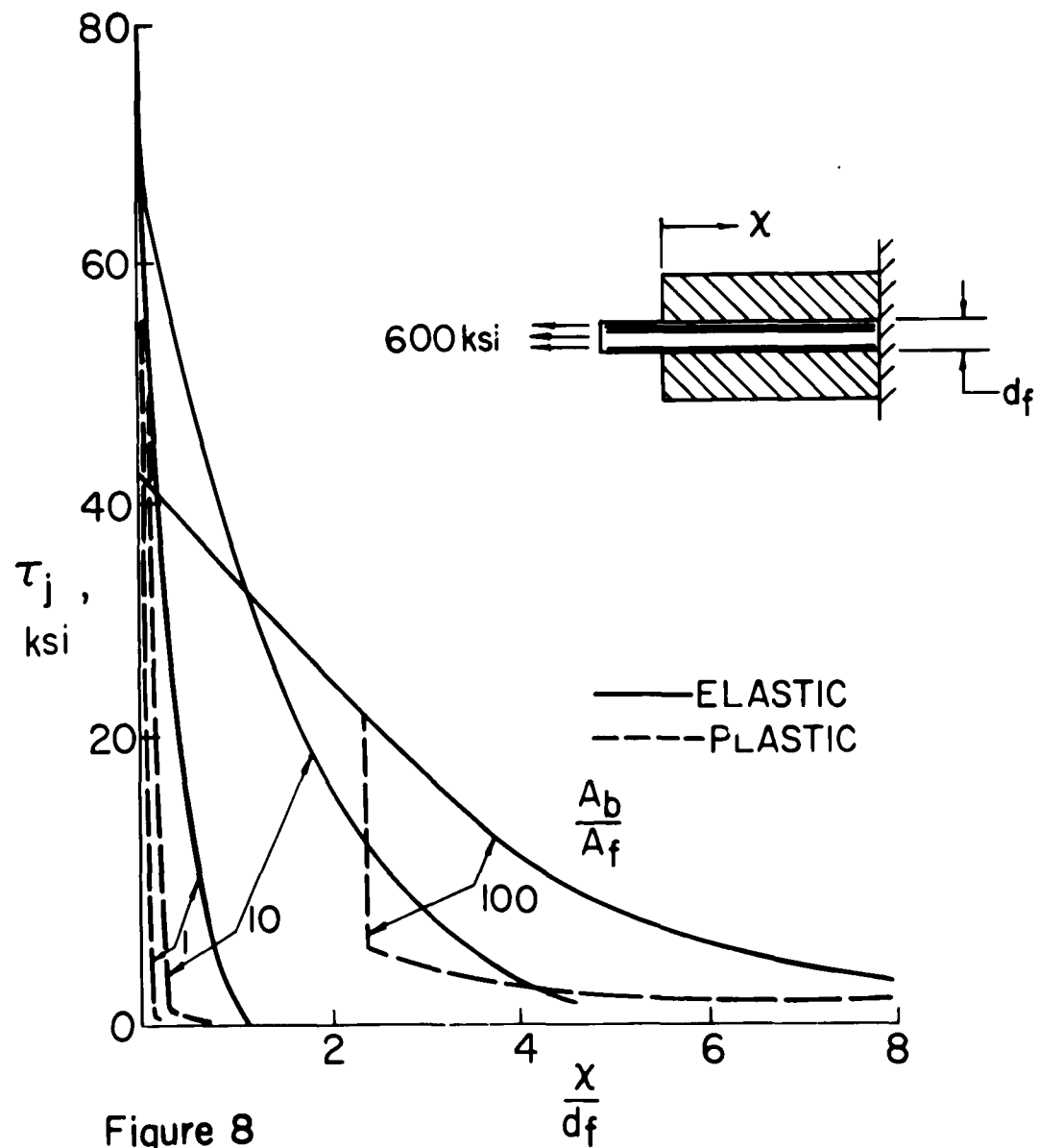APPLIED TO FILAMENT (BINDER ELASTIC,
OR AS IN FIGURE 7)

Figure 8

CALCULATED TENSILE STRESSES σ_f INDUCED IN Al_2O_3 FILAMENT BY TENSION APPLIED TO ELASTIC, COMPOSITE Al-Al_2O_3 BINDER HAVING E_b = 60,000 ksi
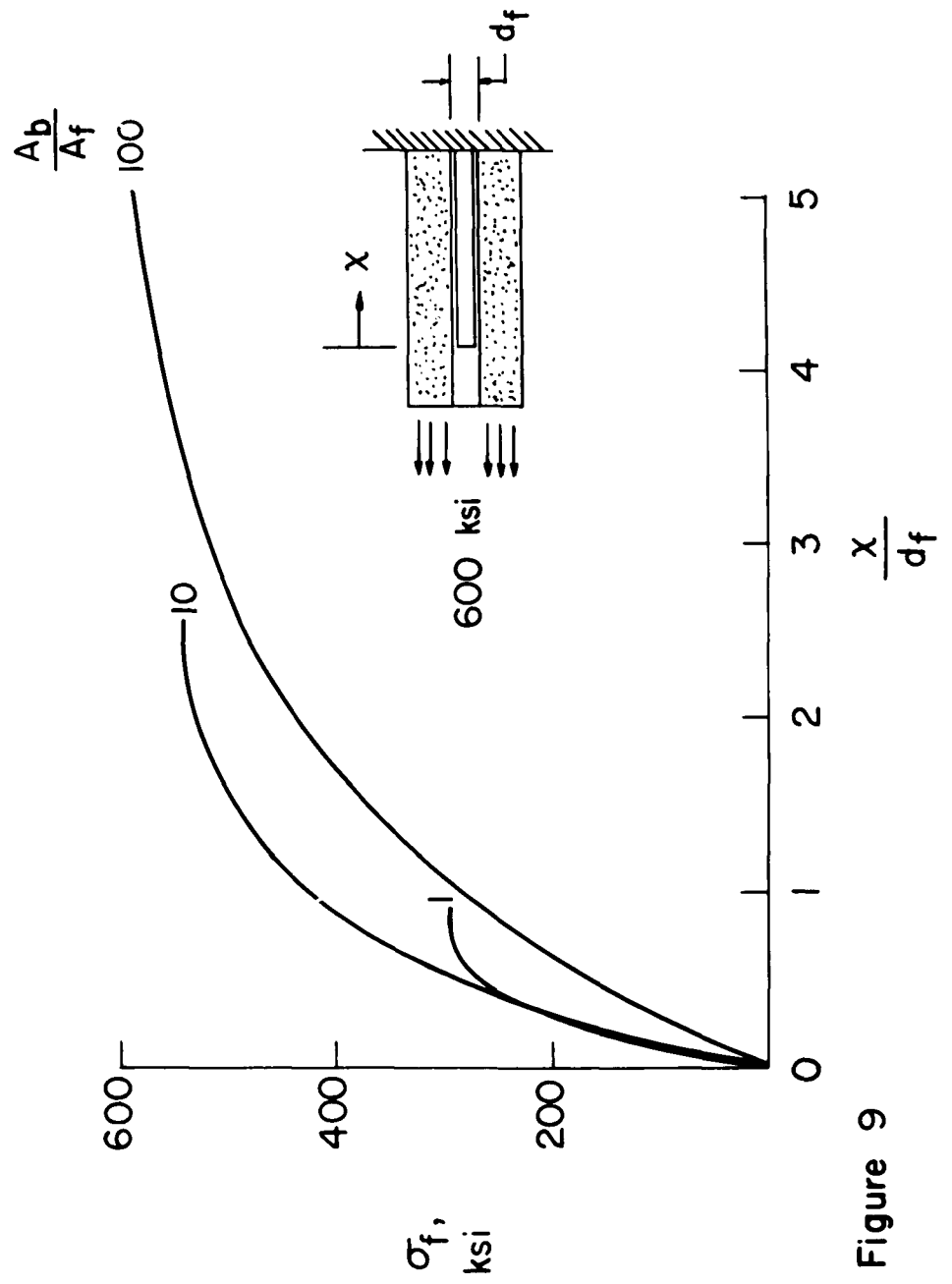
Figure 9

CALCULATED TENSILE STRESSES σ_b INDUCED IN COMPOSITE AI-AI$_2$O$_3$ BINDER HAVING E_b = 60,000 ksi BY TENSION APPLIED TO AI$_2$O$_3$ FILAMENT
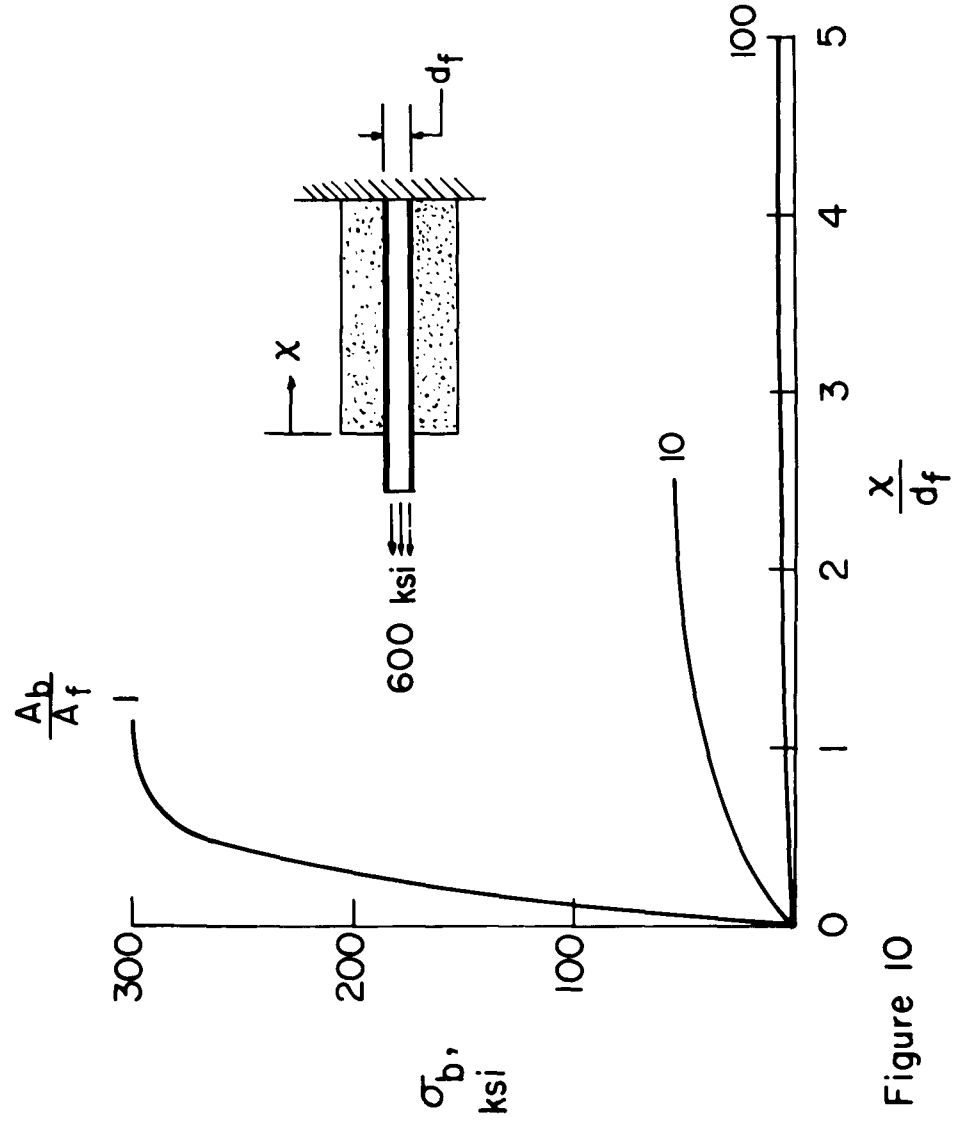

Figure 10

CALCULATED SHEAR STRESSES τ_j OR $-\tau_j'$ INDUCED BETWEEN FILAMENT AND BINDER IN Al-Al$_2$O$_3$ COMPOSITE WITH $E_f = E_b = 60,000$ ksi, LOAD APPLIED TO FIBER OR BINDER
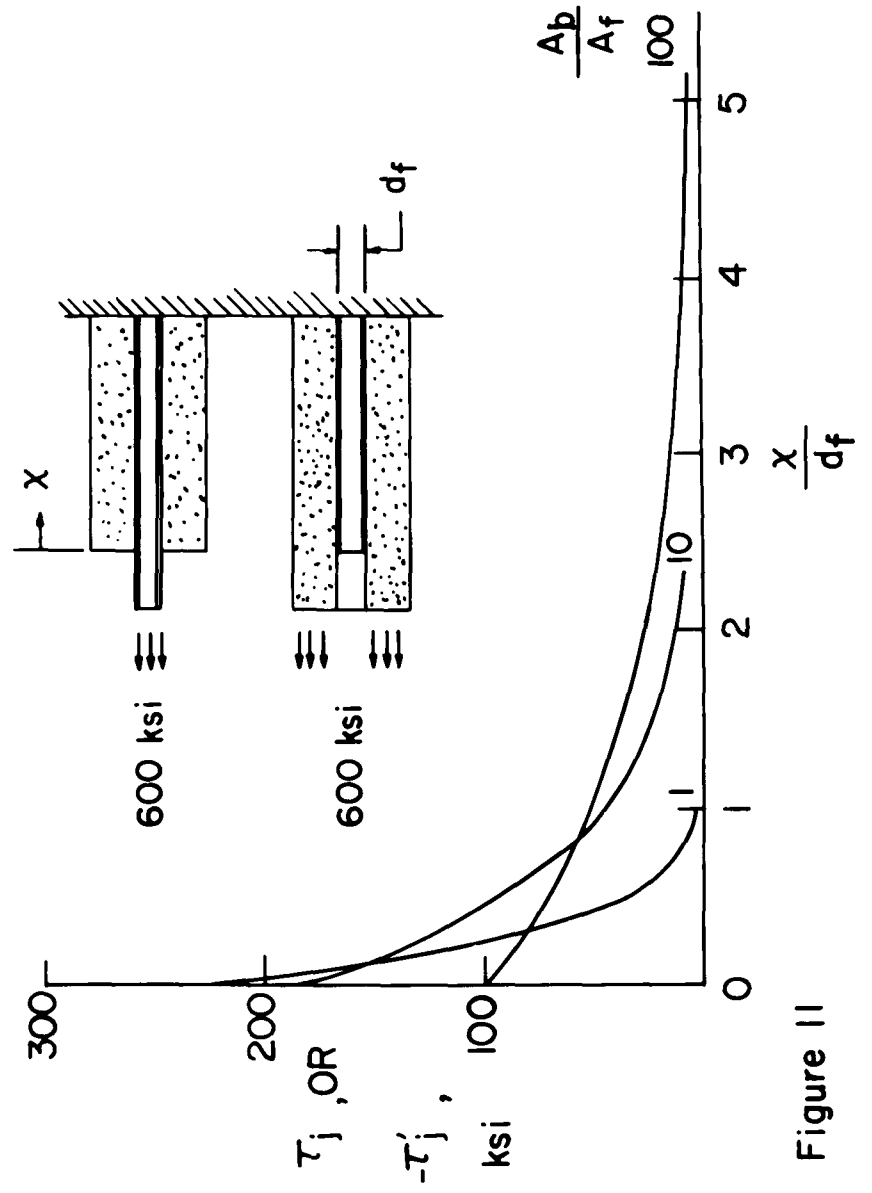

Figure 11

VARIATION OF PARAMETER λ WITH CHANGES IN RELATIVE STIFFNESSES AND PROPORTIONS OF COMPOSITE
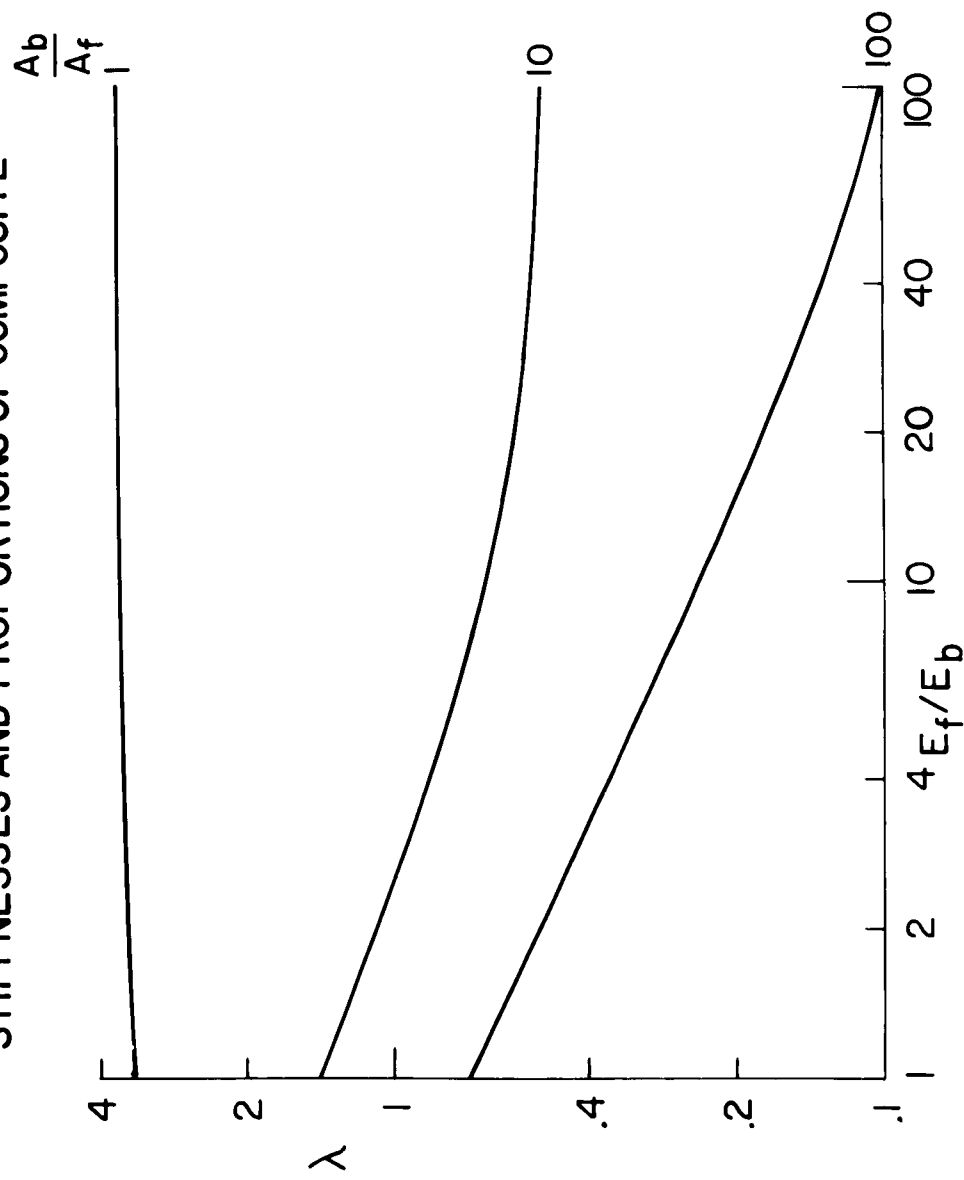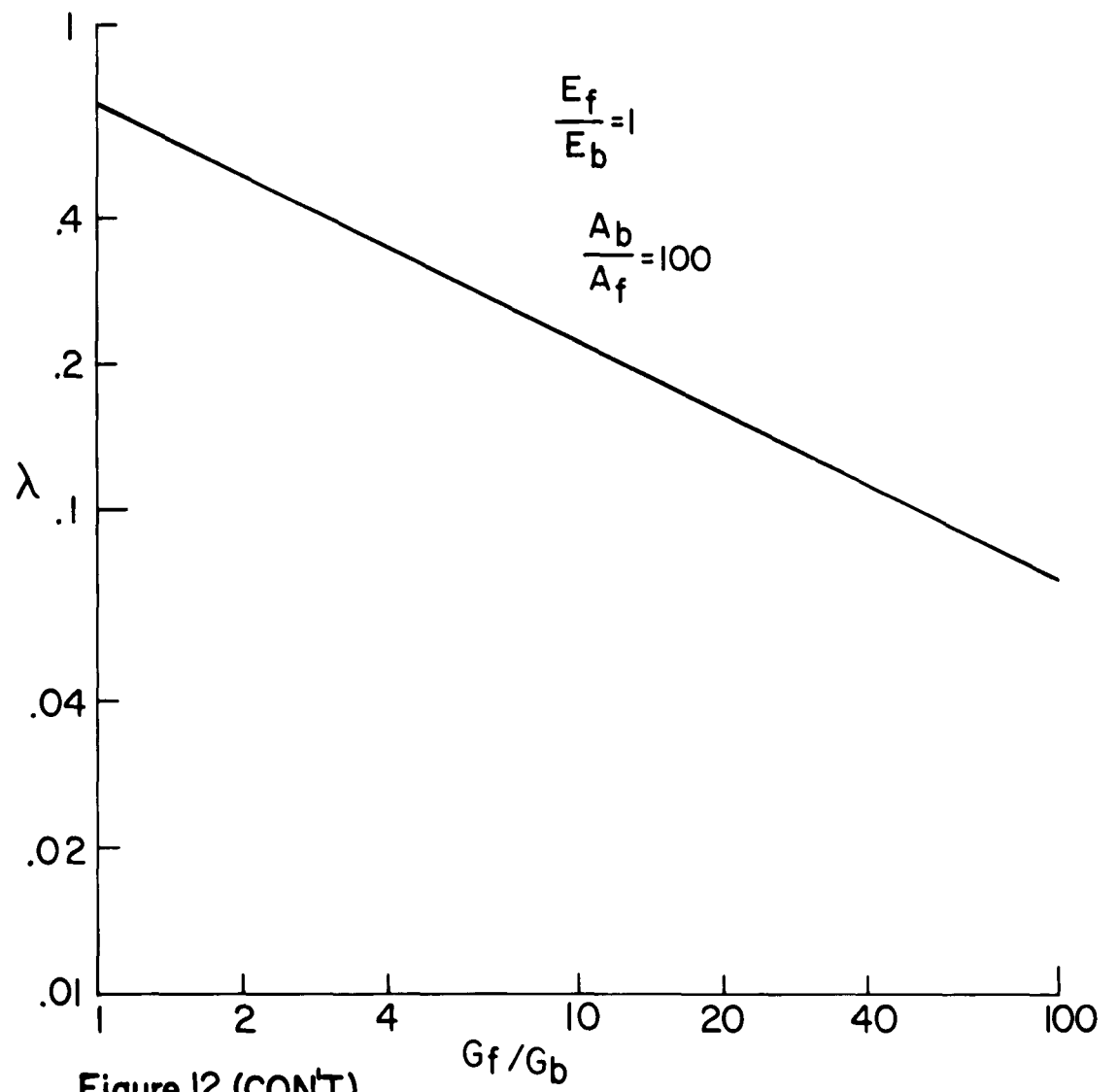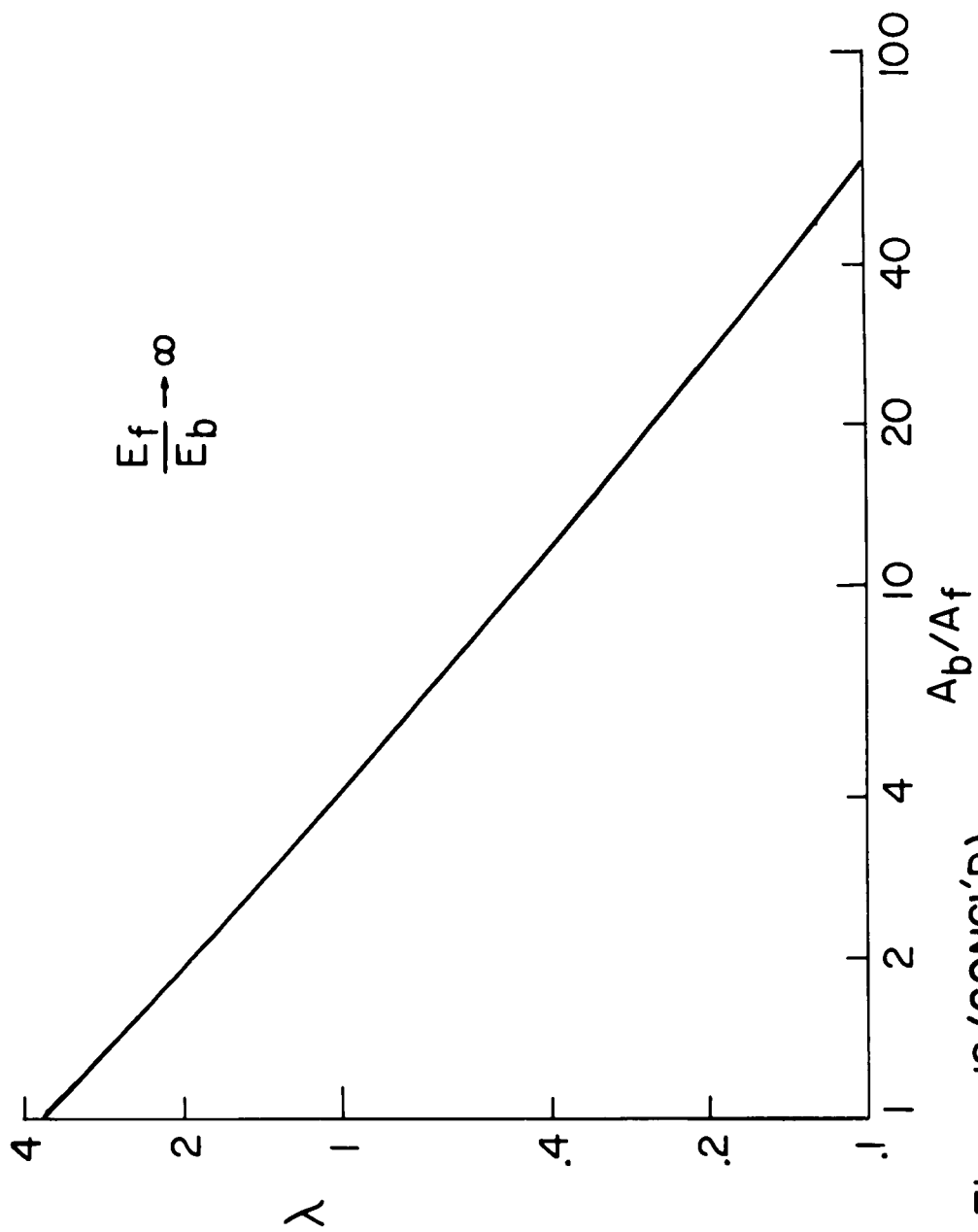
Figure 12

-40-

Figure 12 (CON'T)

Figure 12 (CONCL'D)

DISTRIBUTION LIST

1-4   Department of the Navy   Attn: Mr. John Wright
      Bureau of Naval Weapons
      Munitions Building
      Washington 25, D.C.

5   Wright Air Development Div.   Attn: Mr. R.C. Tomashot
      Nonmetallic Materials Lab
      Wright-Patterson Air Force Base, Ohio

6   Wright Air Development Div.   Attn: Commander WWRNRE-4
      Wright-Patterson Air Force Base, Ohio

7   H. I. Thompson Fiberglas Co.
      1733 Condoza Street
      Los Angeles 7, California

8   Defense Material Center
      Battelle Memorial Institute
      505 King Avenue
      Columbus, Ohio

9   Boeing Airplane Co.   Attn: Mr. P.H. Entz
      Aerospace Div.
      Seattle 24, Washington

10   Thiokol Chemical Corp.   Attn: Mr. James J. Shyne
      Reaction Motors Div.
      Denville, New Jersey

11   Cornell Aeronautical Lab, Inc.
      P.O. Box 235
      Buffalo 21, New York

12   Hughes Aircraft Co.   Attn: Mr. L. E. Gates, Jr.
      Culver City, California

13   Applied Materials Physics Div.   Attn: Mssrs. O. Trout/P. Hill
      Langley Research Center
      National Aeronautics and Space
      Administration
      Langley, Virginia

14   Naval Research Laboratory   Attn: Mr. J.A. Kies
      Washington 25, D.C.   Code 6210

15 Thiokol Chemical Corp.   Attn: Miss M. Becker
   Reaction Motors Div.   Librarian
   Denville, New Jersey

16 Prof. H. T. Corton
   Dept. of Theoretical and Applied Mechanics
   University of Illinois
   Urbana, Illinois

17 Texaco Experiments, Inc.   Attn: Mr. Claude Tally
   Richmond, Virginia

18 Jet Propulsion Lab   Attn: Dr. L. Jaffe/P. J. Schlicta
   California Institute of Technology
   4800 Oak Grove Drive
   Pasadena, California

19 Mr. P. A. Hessinger
   National Beryllia Corp.
   First & Haskell Avenue
   Haskell, New Jersey

20 George Mandel, Chief, Library
   National Aeronautics & Space Administration
   Lewis Research Center
   21000 Brookpark Road
   Celveland 35, Ohio

21 R. Anderson
   National Aeronautics & Space Administration
   Langley Research Center
   Langley, Virginia

22 R. H. Raring
   National Aeronautics & Space Administration
   1512 "H" Street, N. W.
   Washington, D. C.

23 H. Hessing
   National Aeronautics & Space Administration
   1512 "H" Street, N. W.
   Washington, D. C.

24 W. Micks/L. Kaechle
    Rand Corp.
    1700 Main Street
    Santa Monica, California

25 B. Daniels
    Midwest Research Institute
    425 Volker Blvd.
    Kansas City, Mo.

26 Prof. R. Ford Pray
    Syracuse University
    Syracuse, New York

27 I. Perlmutter
    Wright Air Development Div.
    Wright-Patterson Air Foce Base, Ohio

28 L. Hjelm
    Wright Air Development Div.
    Wright-Patterson Air Force Base, Ohio

29 G. Peterson, WWRCNC-1
    Wright Air Development Div.
    Wright-Patterson Air Force Base, Ohio

30 D. Schmidt, WWRCBC-2
    Wright Air Development Div.
    Wright-Patterson Air Force Base, Ohio

31 J. D. Walton, Jr.
    Head - Ceramics Branch
    Georgia Institute of Technology
    Atlanta 13, Georgia

32- Chief
43 Bureau of Naval Weapons, Code D LI-3
    Washington 25, D.C. (10 to ge forwarded to Astia after clearance)

44 Stanford Research Institute   Attn: F.A. Halden
    Menlo Park, California   Ceramics Research Section

45 Cornell University   Attn: E. Scala
    College of Engineering
    Ithaca, New York

46   Owens-Corning Fiberglass Corp.   Attn: R.J. Weaver
      806 Connecticut Avenue, N.W.
      Washington 6, D.C.

47   Prof. E. Machlin
      Materials Research Corp.
      47 Buena Vista Avenue
      Yonkers, New York

48   New England Materials Laboratory, Inc.
      P.O. Box 128
      35 Commercial Street
      Medford 55, Mass.

49   Mr. George Darcy
      Ordnance Materials Research Office
      Watertown Arsenal
      Watertown, Mass.

50   Mr. Morton Kliman
      Chief Ceramics and Sintered Metals Branch
      Rodman Laboratory, Watertown Arsenal
      Watertown, Mass.

51- Chemical Propulsion Information Agency
53   The Johns Hopkins University
      Applied Physics Laboratory
      8621 Georgia Avenue
      Silversprings, Maryland

54   U. S. Army
      Watervliet Arsenal
      Watervliet, New York
      Attention: Lt. Michael Salkind

<u>Missile and Space Division</u>

<u>Valley Forge</u>

L. McCreight	Rm. M9533
W. Sutton	M9124 (50)
E. Feingold	M9120
D. Flom	M9157A
P. Gorsuch	M9138
G. Bainton	M9151
P. Zavitsanos	M9537
N. Dow	Bldg. 5
L. Steg	M9551
R. Cree	M9111
J. Gebhardt	M9130
A. Harrison	U1240 (2)
V. DeSantis	M9132
J. Chorné	M9124
J. Berry	M9132
Documents Library	L1343 (10 + tissue)
B. W. Rosen	M1047
H. Morgan	M3217
J. Dunbar	U4223
H. Rauch	U8417
O. Read	M3134
A. Gatti	M9124
S. Voltz	M9114
N. Dow	Bldg. #5 (25)

<u>Girard Bldg.</u>

I. Gruntfest   Rm. 0813

<u>Burlington, Vermont</u>

W. Barry

<u>Research Laboratory, Schenectady</u>

J. Burke, Main Bldg., Rm. 3019
H. C. Pollock, Radiation Bldg.
W. R. Hibbard, Main Bldg., Rm. 3A18

<u>Major Appliance Laboratory</u>
<u>Appliance Park, Louisville, Ky.</u>

R. Hadley (Met & Ceramics Dept.)

ATL, Schenectady

J. Palm, Bldg. 37, Rm. 2083
T. Jordan, Bldg. 258
H. Plant, Bldg. 258

Lamp Glass Dept., Nela Park
Cleveland 21, Ohio

W. S. Powley, Glass Tech. Lab., Eng. Sec.
W. Louden, Glass Tech. Lab., Eng. Sec.
H. Lettner, Glass Tech. Lab., Eng. Sec.
K. Scott, Glass Tech. Lab., Eng. Sec.

Large Jet Engine Dept., Cincinnati

W. Knaus, Bldg. 501
Applied Mech, CDO

Flight Propulsion Laboratory Dept.
Evendale, Ohio

J. Clark, Alloys Stud. Unit,
Metallurgical Eng. ARO, Bldg. 200

Vallecitos Atomic Laboratory
P.O. Box 846, Pleasanton, Calif.

A. Holden, Metallurgy & Ceramics

Hanford Laboratory, Richland, Wash.

L. Mills, Ceramic Fuel Dev. Oper.

Electronics Park Library, Syracuse

C. Lukens, Bldg. 3, Rm. 143 (1 + 3 TIS pgs)

G.E. Tempo Library (4)
735 State St.
Santa Barbara, Calif.

G.E. Technical Data Center (2 + 6 TIS pages)
Bldg. 5, Rm. 363, One River Road
Schenedtady, N. Y.

G. E. - HMED
Court St., Syracuse, N. Y.

C. R. Wayne, Bldg. 9, Rm. 31

G. E. Small Aircraft Eng. Dept.
1000 Western Ave., West Lynn 3, Mass.

Technical Library

G. E. Com. Sys. Div., Box 2500
Daytona Beach, Florida

P. H. Wagner

Young & Rubicam, Inc.
285 Madison Ave.
New York 17, New York
Attn: Gerald Siesfeld

Div. of Aeronautical Sciences
Univ. of California
Berkeley, California
Attn: Dr. A. K. Oppenheim

UCLA
Dept. of Engineering
Los Angeles 24, California
Attn: C. T. Leondes, Prof. of Eng.

ASTIA (10)
Arlington Hall Station
Arlington 12, Virginia
Attn: TIPCR

GENERAL ⊛ ELECTRIC

SPACE SCIENCES LABORATORY
MISSILE AND SPACE DIVISION

TECHNICAL INFORMATION SERIES

AUTHOR	SUBJECT CLASSIFICATION	NO.
N.F. Dow	COMPOSITE MATERIALS	R63SD61
		DATE August 1963

TITLE Study of Stresses Near a Discontinuity in a Filament - Reinforced Composite Metal	**G. E. CLASS** I
	GOV. CLASS None

REPRODUCIBLE COPY FILED AT MSD LIBRARY, DOCUMENTS LIBRARY UNIT, VALLEY FORGE SPACE TECHNOLOGY CENTER, KING OF PRUSSIA, PA.	**NO. PAGES** 42

SUMMARY

A study is made of stresses in the vicinity of discontinuities in filaments in filament-reinforced, composite materials. Formulas are derived for the calculation of local stresses in filament or binder, and for the shear stresses induced between them. Sample calculations (in both elastic and plastic stress ranges) show that disturbances from the general stress level are primarily local, near the discontinuity, and particularly that the shear stress between fiber and binder is apt to rise to a high peak value at the discontinuity. The magnitude of this peak is shown to be governed by a parameter λ, defined in the report, which also governs the length of filament required to approach infinite length in effectiveness. Thus any attempts to reduce the shear stress, as by permitting yielding of the binder, will also increase the filament length required for effective reinforcement. The conclusion is reached that the accommodation of the high peak shear stresses at discontinuities may well be the crux of the attainment of the potentials apparently available with high-strength filaments or "whiskers" as reinforcements for composite materials.

By cutting out this rectangle and folding on the center line, the above information can be fitted into a standard card file.

AUTHOR _Norris F. Dow_

COUNTERSIGNED _F. W. Wendt_